Journal of Molecular Modeling (2023) 29:230
https://doi.org/10.1007/s00894-023-05624-2

ORIGINAL PAPER

Proton transfer between sulfonic acids and various propylamines by density functional theory calculations

Irina V. Fedorova[1] · **Lyubov P. Safonova**[1]

Received: 29 May 2023 / Accepted: 16 June 2023 / Published online: 5 July 2023
© The Author(s), under exclusive licence to Springer-Verlag GmbH Germany, part of Springer Nature 2023

Abstract

Context Proton transfer in acid–base systems is not well understood. Some acid–base reactions do not proceed to the extent that is expected from the difference in the pK_a values between the base and acid in aqueous solutions, yet some do. In that regard, we have computationally studied the process of proton transfer from the acids of varying strength (benzenesulfonic acid (BSu), methansulfonic acid (MsO), and sulfuric acid (SA)) to the amines with different numbers of propyl substituents on the nitrogen atom (propylamine (PrA), dipropylamine (DPrA), and tripropylamine (TPrA)) upon complexation. Density functional theory calculations were used to thoroughly examine the energetic and structural aspects of the molecular complexes and/or ionic pairs resulting from the acid–base interaction. The potential energy curves along the proton transfer coordinate in these acid–amine systems were analyzed. The change in free energies accompanying the molecular complexes and ionic pair formations was calculated, and the relationship between the energy values and the ΔPA parameter (difference in proton affinity of the acid anion and amine) was established. The larger ΔPA values were found to be unfavorable for the formation of ionic pairs. Using structural, energy, QTAIM, and NBO analyses, we determined that the hydrogen bonds in the molecular complexes PrA-MsO and PrA-BSu are stronger than those in their corresponding ionic pairs. The ionic pairs with the TPrA cation possess the strongest hydrogen bonds of all the ionic pairs being studied, regardless of the anion. The results showed that hydrogen bonding interactions in the molecular complexes contribute significantly to the energies of the acid–base interaction, while in the ionic pairs, the most important energy contribution comes from Coulomb interactions, followed by hydrogen bonding and dispersion forces. The ionic pairs with propylammonium, dipropylammonium, and tripropylammonium cations have stronger ion–ion interactions than tetrapropylammonium (TetPrA)-containing ionic pairs with the same anions. This effect rises with the order of the cation: TetPrA → TPrA → DPrA → PrA, and the sequence of anions is SA → BSu → MsO. The results obtained here expand the concept of acid–base interaction and provide an alternative to experimental searches for suitable acids and bases to obtain new types of protic ionic liquids.

Methods All quantum-chemical calculations were carried out by using the DFT/B3LYP-GD3/6-31++G(d,p) level as implemented in the Gaussian 09 software package. For the resulting structures, the electron density distribution was analyzed by the "atoms in molecules" (QTAIM) and the natural bond orbital (NBO) methods on the wave functions obtained at the same level of theory by AIMAll Version 10.05.04 and Gaussian NBO Version 3.1 programs, respectively.

Keywords DFT calculations · Proton transfer · Proton affinity · Structure · Interaction · Sulfonic acids · Propylamines

Introduction

Salts or ionic liquids with melting points below 100 °C, or below the boiling point of water, are very promising but far from being fully studied. Unlike molecular liquids, which are composed of neutral particles, the particles of ionic liquids carry electrical charges. Ionic liquids are often called "designer solutions" because altering the cation and anion types in their composition as well as changing the length, branching, and functionalization of the alkyl chain enable

✉ Irina V. Fedorova
fiv@isc-ras.ru

[1] G.A. Krestov Institute of Solution Chemistry of the Russian Academy of Sciences, 1 Akademicheskaya Street, Ivanovo 153045, Russia

the synthesis of the salts with different physical and chemical properties for a particular application [1–3]. Of notable interest here are the proton ionic liquids (PILs) as a subclass of ionic liquids due to the fact that they contain an active (reactive/transferring) proton, which determines their high proton conductivity and allows them to be used in the creation of proton-conducting membranes for hydrogen fuel cells [4–6].

As protic ILs are formed by the proton transfer from a Brønsted acid (AH) to a Brønsted base (B) [7, 8], there is a possible equilibrium that can return the components to the neutral particles. The proton transfer equilibrium can be represented by the following equation: acid (AH) + base (B) <=> AH...B <=> A^-…BH^+ <=> A^- + BH^+, corresponding to the molecular complex, neutral ionic pair, and dissociated ions. PILs are often a mixture of ionic and molecular particles. The more the equilibrium shifts to the right, the more ions are in the mixture. Because the properties of PILs are largely dependent on their degree of ionization, most researchers are interested in predicting what type of particles will form when selected bases and acids interact with one another: molecular acid–base complexes, cation–anion pairs, or a mixture of both.

According to numerous studies [9–14], the degree of ionization in the PIL can correlate with the difference in the proton dissociation constants (ΔpK_a) between the base and acid in aqueous solution. Using the ΔpK_a data calculated for 6465 crystalline complexes in the Cambridge Structural Database, Cruz-Cabeza [9] stated that the $\Delta pK_a = 4$ is enough for complete proton transfer from the acid to the base and the formation of the PIL ions. Yoshizawa et al. [10] demonstrated that PILs can be formed only if the ΔpK_a value is higher than 10. Miran et al. [12] concluded that the PIL formed will have the highest ionicity if the ΔpK_a value is higher than 15. In that context, larger ΔpK_a values are advantageous because of the increased proton transfer. When ΔpK_a is small, a certain fraction of the particles remains neutral, which is certainly not desirable for the PILs. Despite this, Stoimenovski et al. [13] reported that ionicity and proton transfer from acetic acid to primary and tertiary amines with similar pK_a values mainly depend on the structure of the ammonium ions rather than the ΔpK_a. Triethylammonium acetate PIL is only partially ionic, with a majority of neutral particles. In addition, it was noted in ref. [14] that the ionic nature of PIL cannot be rationalized simply through the ΔpK_a because the degree of proton transfer in some acid–base reactions is lower than expected from the pK_a values of the acids and bases that are PIL precursors.

The degree of acid-to-base proton transfer can also be estimated using computational chemistry methods [15–20]. It was found that the difference between the anion and base proton affinities in the gas phase (ΔPA) can serve as an alternative and more suitable indicator of the degree of proton transfer. Based on electronic structure calculations of imidazolium-based PILs with bis(trifluoromethylsulfonyl)imide, mesylate, triflate, acetate, and trifluoroacetate anions, Pant et al. [15] concluded that the proton transfer from the acid to the base takes place only if the ΔPA value is lower than 377 kJ/mol. This calculated threshold ΔPA value is slightly higher than the 360 kJ/mol obtained in ref. [19], which deals with the investigation of a significant number of protic acids and alkylimidazoles as PIL precursors. Analysis of a set of combinations of various alkylamines and acids showed that the acid-to-base proton transfer and the formation of an ionic pair are achieved with ΔPA < 400 kJ/mol (or $\Delta pK_a > 12$) [20].

On the whole, it can be said that the role of computational modeling is enormous, despite the clear priority of experimental research in the field of ionic liquids. The most significant are the computational results that are impossible or extremely difficult to determine by experimental means. Quantum chemical calculations are used to probe the potential energy surfaces for proton transfer in acid–base systems in order to determine not only the equilibrium configurations but also the potential energy barriers for this process [21–25]. Direct calculations of the structure and ion–ion interactions in the ionic pairs enable the identification of unique cation/anion combinations, yielding task-specific PILs. From a computational point of view, these compounds are better described when using an isolated single ion pair approach and density functional theory (DFT) methods, which were employed in the literature to calculate many ionic liquids [22, 25–28].

In this work, we continue to investigate protic ILs based on alkylammonium cations. We recently published a mini review [21] on the structures and physicochemical properties of these PILs by pointing out gaps in the computational and experimental data on the PILs with cations bearing propyl radicals. So far, only PILs containing the propylammonium [26] and tripropylammonium [29] cations and the hydrogen sulfate anion have been studied using the DFT method. The physicochemical properties of tripropylammonium hydrogen sulfate PIL have also been reported [21, 30]. Here, we examine the acid–base interactions of amines having different numbers of propyl substituents on the nitrogen atom (propylamine (PrA), dipropylamine (DPrA), and tripropylamine (TPrA)) with sulfuric (SA), methansulfonic (MsO), and benzenesulfonic (BSu) acids using computational chemistry methods. The study also provides comprehensive details on the compounds formed by this interaction, including their structure and interparticle interactions.

The scientific novelty and practical significance are defined by the fact that this work is the first to conduct a comparative-generalizing study of the structural and energetic characteristics of compounds resulting from acid–base interactions, without which it is impossible to predict the physico-chemical properties of liquids. The results obtained here broaden the concept

of acid–base interaction and provide an alternative to searching experimentally for suitable acids and bases to produce new types of protic ILs. Moreover, as noted above, the existing studies of PILs with cations bearing propyl radicals are limited. Our findings can represent a unique opportunity for the identification of trends between structure and properties in a series of alkylammonium-based PILs when elongating the alkyl radical of a cation.

The main findings of this investigation are presented in three parts. The effects of the acid nature and the hydrogen atom substitution on the nitrogen atom in the amine during the process of the acid-to-base proton transfer will be examined first, followed by a discussion of the structures formed by the interaction between the acid and the amine. Second, we will try to shed some light on the quantum nature of hydrogen bonding interactions in the resulting structures. Third, we will estimate the strength of individual hydrogen bonds and their contribution to the total interaction energy. These data were all first-time acquisitions.

Computational methods

The structures of all the compounds presented in this work were obtained with the B3LYP-GD3 functional and 6-31++G(d,p) basis set using Gaussian 09 software [31] via full geometry optimization in the gas phase. The amine and acid molecules at their lowest energies were used to construct the initial structures of different configurations in the acid–amine systems. As a result of acid–base interactions, several configurations of the molecular complexes and ionic pairs were obtained. Frequency calculations were done in order to verify that the obtained geometries are true minima with no imaginary frequencies and to evaluate their thermodynamic characteristics. The structures that best reflect energetically preferred configurations and thermodynamic stability are shown in Fig. 1 below.

The proton affinities of amines and acid anions were determined as the difference between the enthalpy values of the cations and acids and their corresponding amines and anions.

The proton transfer potential energy curves in the acid–amine systems were obtained by the method of scanning proton transfer coordinate along the potential energy surface (PES) as implemented in Gaussian 09. In all cases, a hydrogen atom was shifted from the oxygen atom in hydroxyl group of sulfonic acid to the nitrogen atom of amine with an increment of 0.05 Å. This can schematically be represented as

$$O_{acid}\text{–}H \cdots N_{amine}$$
$$\leftarrow r_1 \rightarrow \leftarrow r_2 \rightarrow$$

At each point of the scan, the transition state structure was optimized without any constraint. The energies associated with proton transfer were calculated from the energy difference between the transition structure with the r_i and δ_i parameters and the global minimum structure (r, δ). The calculation formula is as follows $\Delta E = E_i(R_i, \delta_i) - E(R, \delta)$. The proton transfer coordinate was represented by the value δ that was calculated by the following relation $\delta = r_1 - r_2$.

The possibility of formation of different hydrogen-bonded structures in the acid–amine systems in terms of the standard Gibbs free energy at 298 K was estimated as the difference between the free energy of the compound resulting from the acid–base interaction and the sum of the free energies of the amine and acid molecules.

The interaction energies E_{int} for the molecular complexes were obtained by subtracting the sum of energies of the acid and amine molecules from the total energy of the complex, while the E_{int} values for the ionic pairs were calculated by subtracting the sum of energies of the cation and anion from the total energy of the ionic pair. The binding energies E_{bind} were determined in the same way, but in this case, the energies of separately optimized molecules and ions were used. The difference between binding and interaction energies is the deformation energy E_{def}, the energy required to distort the two molecules (or two ions) from their isolated geometry to that adopted in the complex structure. Both E_{bind} and E_{int} were corrected from the basis set superposition error (BSSE) using the full counterpoise technique of Boys and Bernardi [32].

Topological analysis of electronic density (quantum theory of atoms in molecules (QTAIM)) was performed based on the B3LYP-D3/6-31++G(d,p) wave function in the optimized geometries using the software package AIMAll (version 10.05.04) [33]. Natural bond orbital (NBO) analysis was carried out using the NBO (version 3.1) program [34], which is a component of the Gaussian 09 program [31].

Results and discussion

Formation of neutral molecular complexes and/or ionic pairs

The interaction of the alkylamines—PrA, DPrA, and TPrA—with the selected sulfonic acids—MsO, SA, and BSu—results in the formation of the structures shown in Fig. 1, where we have highlighted the geometric characteristics of hydrogen bonds (proton acceptor distance and bond angle). And it is worth paying attention to some moments here. When the amines considered in this work interact with sulfuric acid, the hydroxyl proton in the acid migrates to the nitrogen atom of the amine, thus enabling the formation of the cation and anion. The NH proton-donating group in the cation is involved in hydrogen bonding to the oxygen atom of the anion, and this in turn leads to the formation of the hydrogen-bonded cation–anion pairs (structures **1a–1c** in Fig. 1). For these ionic pairs, the H…O distances in the N–H…O motifs are larger than the N–H ones, which are ~ 1.1 Å.

It can also be seen from Fig. 1 that the only hydrogen-bonded ionic pairs are formed by the interaction of MsO and

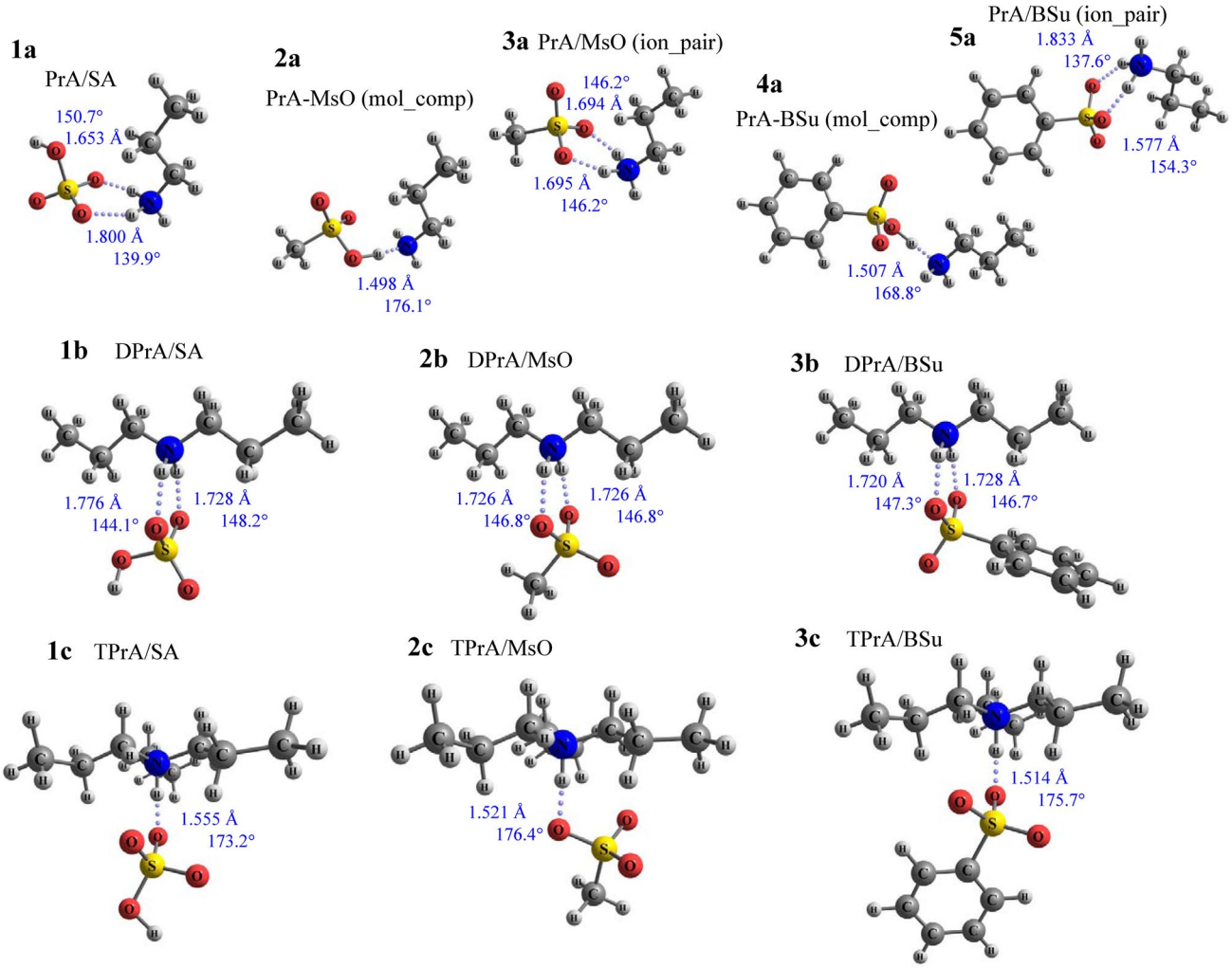

Fig. 1 Calculated structures of the ionic pairs of propylammonium (1a, 3a, 5a), dipropylammonium (1b–3b), and tripropylammonium (1c–3c) cations with hydrogen sulfate, mesylate, and besylate anions, and molecular complexes of propylamine with methanesulfonic (2a) and benzenesulfonic (4a) acids. The structure of the TPrA/SA was taken from our previous work, ref. [29]

BSu with DPrA (structures **2b** and **3b**) and TPrA (structures **2c** and **3c**). The acid–base interactions in the MsO-PrA and BSu-PrA systems, by contrast, lead not only to the formation of the ionic pairs **3a** and **5a** but also to the formation of the molecular complexes **2a** and **4a** (see Fig. 1). For the molecular complex structures, the proton in the O–H…N hydrogen bonding motifs is closer to the oxygen atom of the acid than to the nitrogen atom of the propylamine, i.e., $r_{HO} < r_{HN}$. Initially, we attribute this result to the relatively small strength of these two acids, the pK_a values of which are 0.7 (BSu) [35] and – 1.92 (MsO) [36], as compared with sulfuric acid (pKa = – 3) [37]. In like manner, judging from the pK_a of protonated amines in water [35], propylamine (pK_a = 10.53) is a weaker base than dipropylamine (pK_a = 10.91) and tripropylamine (pK_a = 10.66).

To give a clearer description of the proton transfer process in these acid–base systems, the scanning proton transfer coordinate along the PES in all the acid–amine pairs was performed. The resulting potential energy curves are plotted in Fig. 2. Since a spontaneous proton transfer occurs during the molecular geometry optimizations, it is expected that there is no or a very low energy barrier to this process. Indeed, the potential energy curve for the proton transfer from the SA molecule to the amine in all the systems confirms the hypothesis. Ionic structures with the proton on the amine are clearly the only stable minimum on the PES (Fig. 2a). Similar results are obtained for proton transfer from MsO and BSu to DPrA and TPrA (Fig. 2b). We have not shown the potential energy curves for the acid–DPrA systems because the energy curves for the acid–TPrA systems are the same as those for DPrA cases. Comparing the PES of different systems, it can be found that the energy values associated with proton transfer from the acid to the amine increase in the following order of amines PrA →

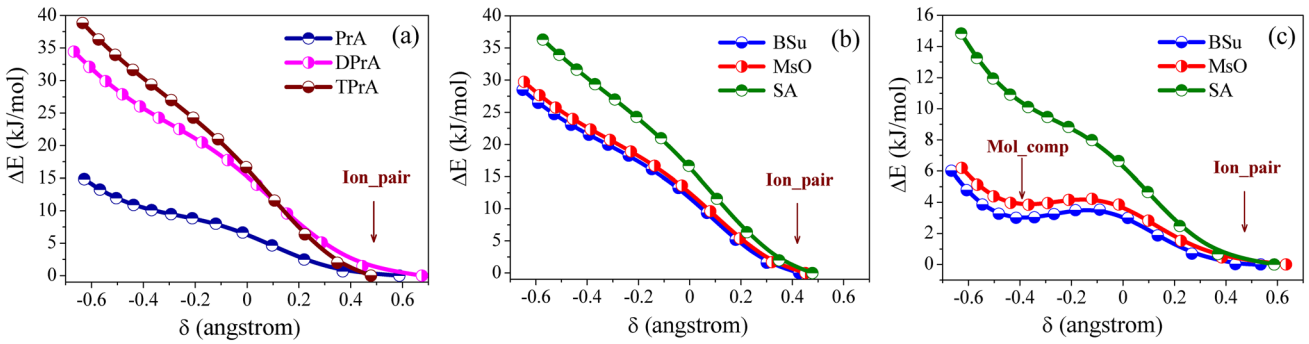

Fig. 2 Potential energy surfaces of sulfuric acid–amine (**a**), acid–tripropylamine (**b**), and acid–propylamine (**c**) systems along the δ coordinate. At each point on the curve, all structural parameters were optimized

DPrA ~ TPrA, as seen in Fig. 2a, which is also consistent with the larger base strengths of DPrA and TPrA in comparison with PrA.

The PES for proton transfer from BSu and MsO to the propylamine, in contrast to the previous examples, reveals the energy minimum corresponding to neutral structures **2a** and **4a** with a proton on the oxygen atom of the acid. But in addition to this minimum, another one occurs for the ionic state at the larger value of the OH distance (Fig. 2c). The energy barrier for proton transfer from the acid to the propylamine is equal to 0.52 (BSu) and 0.38 (MsO) kJ/mol. This extremely low energy barrier, which is even lower than the RT value at 298 K (< 2.5 kJ/mol), could not prevent the spontaneous proton transfer during the acid–amine interaction. This suggests that the acidic proton will easily pass through this minimal barrier just by means of thermal motion. Figures 2b and 2c also show that the energy proton transfer in the studied systems increases with the order of acids BSu ~ MsO → SA. This sequence correlates well with an increase in the proton donor ability pK_a of these acids.

For the tested systems, it is possible to discuss the process of proton transfer between the acids and amines in terms of Gibbs free energy change (ΔG_{298}) reported in Table 1. The ΔG_{298} values calculated for the complexes and ionic pairs in Fig. 1 are all negative, indicating that their formation processes take place. The ΔG_{298} values for the molecular complexes PrA-BSu and PrA-MsO are somewhat more negative than for their corresponding ionic pairs PrA/BSu and PrA/MsO. The formation of the molecular complexes of these acids with the propylamine is thus more thermodynamically favorable than the cation–anion pairs. It is evident that the strong Coulomb interaction between the positively charged cation and the negatively charged anion in these ionic pairs leads to a reduction in hydrogen bond distance to such a degree that back proton transfer becomes preferred during the gas phase optimization, thus favoring the formation of neutral particles. A similar phenomenon was observed for many acid–base systems,

Table 1 Gibbs energy change ΔG_{298} of the formation of the molecular complexes and ionic pairs. The numbers given in parenthesis refer to the proton affinities of amines and acid anions. All values are quoted in kJ/mol

Amines	Acids		
	SA (1290.34)	MsO (1330.64)	BSu (1319.72)
PrA (916.76)	− 53.23	− 37.01 (mol_comp)	− 35.72 (mol_comp)
		− 33.06 (ion_pair)	− 34.78 (ion_pair)
DPrA (960.96)	− 76.32	− 53.91	− 54.75
TPrA (991.63)	− 78.99	− 55.60	− 59.91

especially imidazole- and trimethylethylamine-based ones [38]. It is also noted that the acids that are more likely to exhibit the ability to form molecular complexes during gas-phase optimizations are hydrochloric, methansulfonic, trifluoromethanesulfonic, and trifluoroacetic acids.

The Gibbs energies of ionic pair formations increase along the order PrA → DPrA → TPrA, with the sequence of anions being MsO~Bsu → SA (see Table 1, Fig. 3). Since all the calculations are performed in the gas phase, the increase in the ΔG_{298} in the abovementioned series of cations and anions is more closely related to the change in their PA values than to the pK_a obtained in the aqueous solution.

In our previous study [20], using the Gibbs free energies for the optimized gas-phase structures of both cation–anion pairs and acid–base complexes along with their ΔPA values, we found that the ionization by proton transfer and the formation of ionic pairs with the general formula $(R)_nNH_{4-n}/A$ can take place only when the ΔPA value is smaller than 400 kJ/mol. As is revealed from an inspection of Fig. 3a, the results obtained here fit well into these data points, showing that the larger ΔPA values are certainly not desirable for the ionic pair formations. From the obtained new results and in previous sets of data, it is impossible to define a clear relationship between ΔG_{298} and ΔpK_a values because the pK_a values for acids and

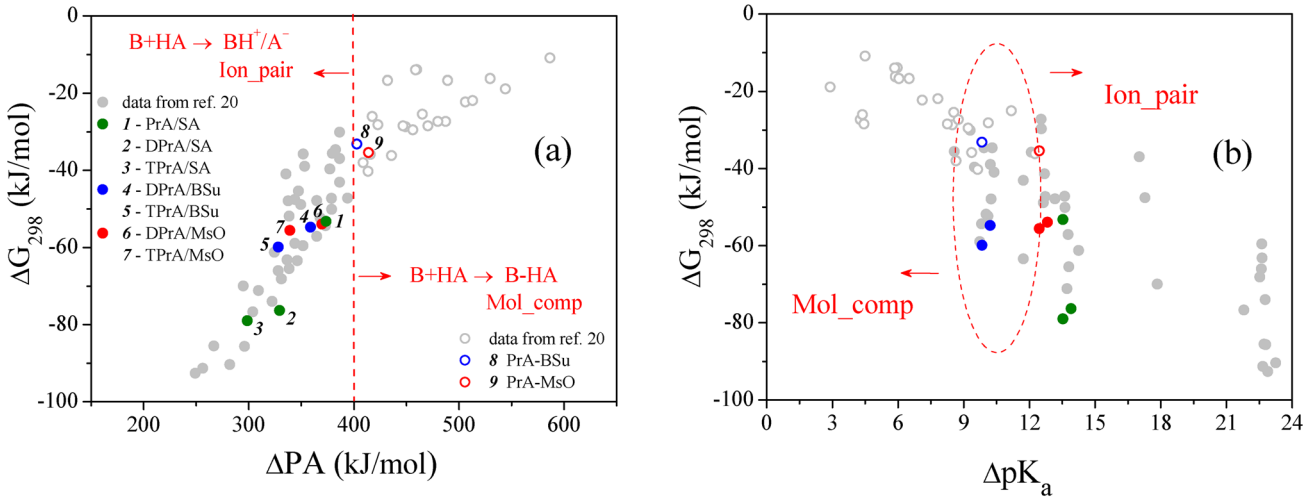

Fig. 3 Change in Gibbs free energies of the formation of molecular complexes and ionic pairs on the ΔPA (**a**) and ΔpK_a (**b**) parameters. All data were obtained from the B3LYP-GD3/6-31++G(d,p) level

bases were determined experimentally and have a certain error in their determination. As shown in Fig. 3b, the data points for the BSu–amine and MsO–amine systems fall into the region of ΔpK_a values in which the molecular complexes together with ionic pairs can coexist. There is, however, a high probability of obtaining fully ionized liquids with SA anion due to the large difference in pK_a values.

Structural features

Let us now discuss the results of quantum chemical calculations of the molecular complexes and ionic pairs, focusing on the characteristics of hydrogen bonds. Since, as mentioned above, the molecular complexes PrA-MsO and PrA-BSu can be transformed into cation–anion pairs, both types of structures were carefully considered. As displayed in Fig. 1, the structures of the molecular complexes PrA-MsO **2a** and PrA-BSu **4a** have only one hydrogen bond between the hydroxyl proton of the acid and the nitrogen atom of the propylamine. The H…N distance in the O–H…N motifs is much shorter than the sum of the Van der Waals radii of the H and N atoms, $\Sigma r_{vdW} = 2.75$ Å [39]. This proves, according to the guidelines set by IUPAC [40], the existence of hydrogen bonds within these complexes. For the complex with MsO, the H…N distance is shorter than that found for the complex with BSu, which is consistent with its acidity strength. The bond angle OHN values are slightly smaller than those of the ideal hydrogen bonding geometry of 180°. Geometrically [41], the (O–)H…N bonds between the acid and the propylamine molecules can be classified as very strong hydrogen bonds with r_{HN} smaller than 1.5 Å.

We note here that the ionic pairs sharing the same alkylammonium cation but different anions have, in general, similar structures, and the cation in each of these ionic pairs exhibits qualitatively similar binding patterns to anions. From the results in Fig. 1, it is seen that the formation of the ionic pairs with PrA cation **1a**, **3a**, and **5a** and those with DPrA cation **1b–3b** is accompanied not only by the transfer of a proton from the acid to the amine, resulting in the formation of two ions as well as a hydrogen bond (N–)H...O, but also by an additional hydrogen bond between the other proton in the cation amino group and the oxygen atom in the acid anion. A similar phenomenon was observed for the ionic pairs with primary (methyl, ethyl, propyl and butyl) and secondary (dimethyl, diethyl, ethylmethyl and dibutyl) ammonium cations and anions of various sulfonic acids [21, 26, 42]. Despite the strong electrostatic force of attraction between ions, these ionic pairs show typical hydrogen bond distances and bond angles as known for hydrogen bonds in molecular liquids [40]. The (N–)H...O bonds in the ionic pairs with PrA and DPrA cations have different lengths, except for PrA/MsO and DPrA/MsO, whose formation results in two structurally equivalent hydrogen bonds. The NHO angles in all the abovementioned ionic pairs are distorted from their linear geometry. Interestingly, the ring structures of dual hydrogen bonds in the ionic pairs with DPrA cation and SA or BSu anion are more symmetrical than those in the ionic pairs with PrA cation, which is seen via the quite close lengths of both hydrogen bonds. The same results were found in Hun's study [26] by comparing the calculated (N–)H…O bond lengths in the ionic pairs composed of primary (ethyl, propyl, isopropyl, and tert-butyl) and secondary (dimethyl and ethylmethyl) ammonium cations paired with SA anion. Our optimized PrA/SA structure does not differ essentially from the geometry obtained in ref. [26] using the B3LYP-D3(BJ)/6-311++(3df,3pd) level, except for the hydrogen bonds, which have slightly shorter distances of 1.651 and 1.728 Å.

Compared to this, a sole (N–)H…O hydrogen bond is formed in the ionic pairs with TPrA cation **1c–3c** (see Fig. 1). In these cases, the bonds are characterized by relatively short distances and the linearity of the N–H…O motifs. Based on Fig. 1, it is seen that the H…O distance increases in the order BSu→MsO→SA, which is inverse to the relative strength of these acids. With geometric criteria, the hydrogen bond in the ionic pairs with the TPrA cation, regardless of the anion, is much stronger in strength than each of the hydrogen bonds in the ionic pairs with the PrA and DPrA cations. For ionic pairs with TPrA cation, some test calculations were carried out by applying wB97X-D level with the same basis set, and no qualitatively different result was observed. The optimized geometries of the investigated systems are quite similar for both methods. At the same time, the B3LYP-GD3 functional predicts lower values of the H…O distances in the hydrogen-bonded fragments than the wB97X-D level (1.530, 1.537, and 1.560 Å for TPrA/BSu, TPrA/MsO, and TPrA/SA, respectively), while the H-bond angle values are close to each other for both methods. We obtained the same trends in the geometric parameters of the hydrogen bonds and energy characteristics in the series of ionic pairs of tripropylammonium-based PILs (at the qualitative level) as B3LYP-GD3 calculations. The results of all these calculations can also be found in Table 2 below.

The analysis of QTAIM and NBO parameters

The presence of hydrogen bonds in the molecular complexes and ionic pairs was verified and analyzed using the QTAIM theory [43–45]. On the basis of this theory, the characteristics of hydrogen bonds at bond critical points (BCPs) can be evaluated in terms of many topological descriptors [21, 27, 46, 47]. The following parameters of the BCPs are considered here: the electron density $\rho(r)$, its Laplacian $\nabla^2\rho(r)$, and the total electron energy density $H(r)$, and these values are summarized in Table 3. The magnitude of the electron density at the BCPs of interacting atoms has a central role in the QTAIM analysis and is quite often used to characterize the strength of bonding interactions. The higher the $\rho(r)$ value at the BCP is, the more the electronic charge is concentrated on the surface at this critical point, making the considered interaction stronger and more covalent. QTAIM allows for the classification of atomic interactions into two

Table 2 Calculated energetic characteristics of the molecular complexes and ionic pairs; the interaction energy E_{int}[a], the binding energy E_{bind}, the deformation energy E_{def}, hydrogen bond energy E_{HB}, and $E_{HB\text{-}Espinosa}$ (all values are in kJ/mol)

Compounds	E_{HB}	$E_{HB\text{-}Espinosa}$	E_{int}	E_{bind}	E_{def}	E_{disp}
PrA-MsO	− 83.16	− 117.18	− 111.76	− 82.30	29.46	− 21.10
PrA-BSu	− 80.97	− 112.54	− 103.26	− 78.68	24.58	− 21.48
PrA/MsO	− 72.46; − 72.32 (− 144.77)	− 50.44; − 50.25 (− 100.69)	− 514.72	− 492.71	22.01	− 23.17
DPrA/MsO	− 67.87; − 67.87 (− 135.74)	− 46.88; − 46.85 (− 93.73)	− 486.31	− 468.44	17.87	− 29.20
TPrA/MsO	− 107.79; − 101.93[a]	− 90.28 − 84.15[a]	− 468.98 − 460.70[a]	− 448.56	20.42	− 37.53
PrA/BSu	− 94.15; − 54.66 (− 148.81)	− 72.49; − 36.80 (− 109.29)	− 503.88	− 478.84	25.04	− 24.10
DPrA/BSu	− 68.56; − 67.45 (− 136.01)	− 47.55; − 46.66 (− 94.21)	− 475.72	− 456.52	19.20	− 36.65
TPrA/BSu	− 109.58 − 103.72[a]	− 92.93 − 86.08[a]	− 457.78 − 448.99[a]	− 433.55	24.23	− 39.83
PrA/SA	− 78.71; − 57.85 (− 136.56)	− 56.01; − 39.03 (− 95.04)	− 487.86	− 468.16	19.70	− 20.89
DPrA/SA	− 68.01; − 61.75 (− 129.76)	− 46.36; − 41.50 (− 87.86)	− 460.27	− 442.20	18.07	− 27.91
TPrA/SA	− 98.87 − 95.45[a]	− 78.89 − 76.14[a]	− 443.71 − 438.02[a]	− 424.15	19.56	− 37.11

The numbers in parenthesis refer to the total energy of two hydrogen bonds

[a]For comparison purposes, our data from the wB97X-D/6-31++G(d,p) calculations were also added

Table 3 QTAIM (electron density at the bond critical point $\rho(r)$ (au), its Laplacian $\nabla^2\rho(r)$ (au), total electron energy density $H(r)$ (au)) and NBO (second order perturbation energy $E^{(2)}$ (kJ/mol) for orbital interaction and charge transfer q_{CT} (ē)) parameters for the hydrogen bonds in the tested complexes and ionic pairs

Compounds	Bond type	$\rho(r)$	$\nabla^2\rho(r)$	$H(r)$	$E^{(2)}$	q_{CT}
PrA-MsO	(O–)H…N	0.0924	0.0473	− 0.0387	326.56	0.182
PrA-BSu	(O–)H…N	0.0901	0.0571	− 0.0357	308.12	0.176
PrA/BSu	(N–)H…O (1)	0.0645	0.1562	− 0.0080	241.32	0.126
	(N–)H…O (2)	0.0361	0.1024	− 0.0012	85.01	0.047
DPrA/BSu	(N–)H…O (1)	0.0461	0.1289	− 0.0020	138.74	0.078
	(N–)H…O (2)	0.0453	0.1270	− 0.0019	134.56	0.075
TPrA/BSu	(N–)H…O	0.0756	0.1678	− 0.0147	311.56	0.169
PrA/MsO	(N–)H…O (1)	0.0489	0.1336	− 0.0025	144.35	0.080
	(N–)H…O (2)	0.0488	0.1333	− 0.0024	144.14	0.080
DPrA/MsO	(N–)H…O (1)	0.0456	0.1267	− 0.0021	136.90	0.075
	(N–)H…O (2)	0.0456	0.1266	− 0.0020	136.69	0.074
TPrA/MsO	(N–)H…O	0.0743	0.1664	− 0.0138	305.93	0.165
PrA/SA	(N–)H…O (1)	0.0534	0.1431	− 0.0035	170.96	0.093
	(N–)H…O (2)	0.0384	0.1094	− 0.0012	94.22	0.050
DPrA/SA	(N–)H…O (1)	0.0457	0.1266	− 0.0018	138.11	0.078
	(N–)H…O (2)	0.0412	0.1155	− 0.0013	112.20	0.060
TPrA/SA	(N–)H…O	0.0679	0.1646	− 0.0095	271.58	0.135

broad categories [48]: (1) shared interactions, such as covalent and polarized bonds with $\rho(r) > 10^{-1}$ a.u. and $\nabla^2\rho(r) < 0$, and (2) closed-shell interactions, such as hydrogen bonds and van der Waals interactions, and in this case $\rho(r)$~10^{-2} a.u. and $\nabla^2\rho(r) > 0$.

In the present study, all the (O–)H…N interactions in the molecular complexes and the (N–)H…O interactions in the ionic pairs are characterized by low $\rho(r)$ and positive $\nabla^2\rho(r)$ values, which are typical of hydrogen-bonded closed-shell interactions. We note that the (O–)H…N interactions in the molecular complexes PrA-MsO and PrA-BSu have the highest $\rho(r)$ values, which are indicative of the strongest hydrogen bonding interactions and the highest covalent character of these interactions compared to the (N–)H…O interactions in the ionic pairs with the corresponding cation and anion.

In all of the ionic pairs with PrA and DPrA cations and the studied anions, with the exception of MsO, the difference in the $\rho(r)$ values at the BCPs of the (N–)H…O bonds clearly reflects their non-equivalence. Herewith, the $\rho(r)$ value of one hydrogen bond when going from the PrA to the DPrA cation in the ionic pairs with the same anion decreases, while this value for another bond increases. This, in turn, reduces the difference between the electron densities on dual hydrogen bonds and leads to a smaller difference in the bond distances, which agrees with a more symmetrical ring structure in the latter. Among all the ionic pairs, the obtained values for electron density at the (N–)H…O BCPs are the largest for the ionic pairs with the TPrA cation, indicating the strongest interaction between the interacting H and O atoms. From the analysis, it can also be concluded that the strength of the hydrogen bonding interactions in the ionic pairs with the TPrA cation increases with the order of anions SA → MsO → BSu. Note that the $\rho(r)$ parameter of hydrogen bonds in all the compounds studied here correlates well with the hydrogen bond distance and is reflected in the exponential decay in Fig. 4a. As is seen, for the ionic pairs, there is a decrease in the electron density at the BCPs of the hydrogen bonds and their strength with increasing H…O distance because the increase in the atomic separation leads to a smaller orbital overlap and decreases the electron density along the bond path. The same is true for the molecular complexes with propylamine, despite the fact that their data fall outside the scope of the general correlation.

In addition, the sign of the total electron energy density $H(r)$ at the BCP can characterize the degree of covalency of the hydrogen bonds [49]. The $H(r) > 0$ denotes weak hydrogen bonding interactions that are mainly electrostatic in nature. When the $H(r) < 0$, the covalent component contributes partially to the hydrogen bond. An analysis of Table 3 reveals that the $H(r)$ at the BCPs is negative in both the molecular complexes and ionic pairs. These observations suggest that all of the considered (O–)H…N and (N–)H…O interactions are rather strong hydrogen bonds with a partly covalent character.

Further information on hydrogen bonding in the molecular complexes and ionic pairs was obtained from NBO analysis [50]. According to the NBO methodology, the formation of the hydrogen bonds denotes that a certain amount of electronic charge is transferred from the proton acceptor lone pairs (LP) to the proton donor antibonding orbital (BD^*). The magnitude of charge transfer (q_{CT}) can be obtained from the following equation $q_{CT} = n \times (F_{ij}/(\varepsilon_i - \varepsilon_j))^2$, where n is the

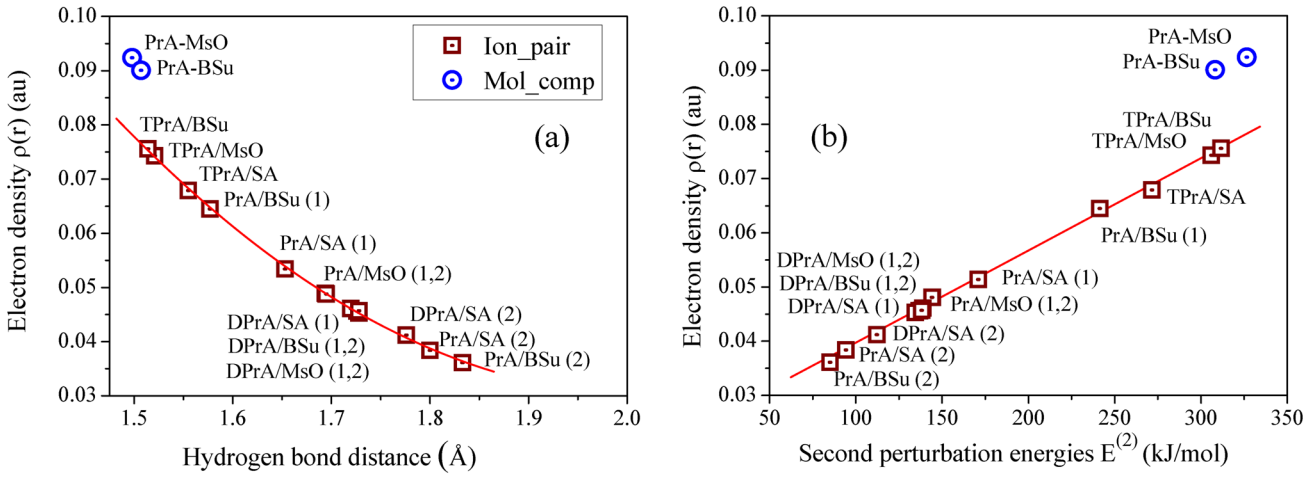

Fig. 4 Electron density versus hydrogen bond distances (**a**, left) and second perturbation energies $E^{(2)}$ (**b**, right) for the studied systems. The numbers in parentheses refer to the numbering of hydrogen bonds

orbital occupancy, F_{ij} is the off-diagonal NBO Fock matrix element, and ε_i and ε_j are the diagonal elements (orbital energies). The interaction energies between the donor and the acceptor NBO orbitals (or stabilization energies, $E^{(2)}$) are calculated by second-order perturbation theory as follows: $E^{(2)} = n \times F^2_{i,j}/(\varepsilon_i - \varepsilon_j)$. The greater the $E^{(2)}$ value is, the more intensive is the donor–acceptor interaction and the stronger is the hydrogen bond.

As given in Table 3, the larger $E^{(2)}$ energy of the orbital interaction $LP_N \rightarrow BD^*_{O-H}$ in complex PrA-MsO implies that the (O–)H…N bond in this complex is stronger than that of complex PrA-BSu, which is in good agreement with the results of the aforementioned geometric and topological analysis of these interactions. If the hydrogen bond is formed within the ionic pairs PrA/MsO and PrA/BSu, the orbital interaction $LP_O \rightarrow BD^*_{N-H}$ is accompanied by a smaller stabilization energy in contrast to their molecular complexes. The $E^{(2)}$ values are very close for both hydrogen bonds in the PrA/MsO as well as in the DPrA/MsO. The formation of hydrogen bonds in the ionic pairs with the same cations but BSu and SA anions leads to an increase in the $E^{(2)}$ values for one of the bonds and a decrease in these values for the other bond. Among the ionic pairs studied, the strongest electron donation occurs from the lone pair orbitals of the oxygen atom of the acid anion to the BD*(N–H) orbital of the TPrA cation. Figure 4b shows the excellent correlation between $E^{(2)}$ for the $LP_O \rightarrow BD^*_{N-H}$ interaction and electron density values in the (N–)H…O BCPs for the examined ionic pairs. The molecular complexes with the $LP_N \rightarrow BD^*_{O-H}$ interactions lie outside of such a relationship. Notably, the charge transfer values for the $LP_N \rightarrow BD^*_{O-H}$ interactions in the molecular complexes and the $LP_O \rightarrow BD^*_{N-H}$ interactions in the ionic pairs are larger in all the cases than the accepted standard for the formation of conventional hydrogen bonds ($q_{CT} \geq 0.01$ ē) [51] indicating that the covalent part of the hydrogen bond is highly stabilizing. The two independent approaches (QTAIM and NBO) employed here are complementary, and together, they provide a more complete understanding of the hydrogen bonding interactions in the studied compounds.

Hydrogen bond energies and stability

In terms of quantum chemical calculations, the interaction energy, which directly reflects the stability of both molecular complexes and ionic pairs, is of special interest. The more negative is the energy value, the more stable is the formed structure. The interaction energies and their components for the investigated complexes and ionic pairs are presented in Table 2.

As is seen, the interaction energies of the molecular complexes are characterized by much lower values than those of the ionic pairs. Obviously, the major energetic difference between the complexes and the ionic pairs is the growing role of Coulomb attraction that ensures stronger interaction in the latter. Among the two complexes under study, PrA-MsO has a slightly larger E_{int} than PrA-BSu, which is also consistent with the sequence of their acid strengths (MsO > BSu). Comparing the E_{int} values for the ionic pairs, it can be immediately seen that the highest energy is registered in all the ionic pairs with the PrA cation. The energy of ion–ion interactions in the ionic pairs with the same anion decreases as the number of propyl groups in the cation (PrA → DPrA → TPrA) increases, owing to weakening Columbic interactions imposed by increased cation size. When going from primary to tertiary ammonium cations bearing methyl, ethyl, or butyl radicals, the ionic pairs with mesylate [42], hydrogen sulfate [42], triflate [21], and trifluoroacetate [52] anions

exhibit the same pattern. And furthermore, for a series of alkylammonium PILs with trifluoroacetate anion, the trends in changes in the geometric parameters of the hydrogen bond and the energy of ion–ion interactions depending on the cation are similar in both the gaseous and liquid phases [52]. After analyzing our results and the literature data [21, 42] on structurally similar alkylammonium-containing ionic pairs with the studied anions, we also reveal that the increase of the alkyl group size in the tertiary cation (TMA < TEA < TPA < TBA) weakens the ion–ion interaction in the ionic pair regardless of the anion. From Table 2, it follows that the replacement of the hydroxyl group in the hydrogen sulfate anion by the benzene ring (Bsu) and methyl group (MsO) in the ionic pairs with the same cation leads to an increase in the energy of ion–ion interactions. This series correlates very closely with the proton affinity of the considered acid anions, showing that the anions with larger PA have a strong tendency to bind with the cation in the ionic pairs. Our calculations show that the TPrA cation interacts far more strongly with all the studied anions in the ionic pairs than with the triflate anion (− 418.15 kJ/mol) [21] and the bis(trifluoromethanesulfonyl)imide anion (− 388.90 kJ/mol) [29], the PA values of which are 1247.94 and 1228.83 kJ/mol, respectively.

It is already well known that the ion–ion interaction in the ionic pairs is definitely stronger in protic ILs than aprotic ILs due to the directional nature of hydrogen bonding, shorter interatomic distances between the ions participating in the hydrogen bonding, and the limited number of hydrogen bonds [21, 38, 53]. To verify these claims, we also performed quantum chemical calculations for the ionic pairs with the tetrapropylammonium cation (TetPrA) in combination with each of the studied anions. Figure 5 depicts the optimized geometries of these ionic pairs. Also given in this figure are hydrogen-bonded distances between the cation and the anion. It is seen that the anion in these ionic pairs forms multiple hydrogen bonding interactions with the hydrogen atoms in the propyl chains of the cation. All of the (C–)H…O bonds, however, have interatomic distances greater than 2 Å and are closed-shell weak interactions ($\nabla^2\rho(r) = 0.0461–0.0257$ au and $H(r) = 0.0001–0.0012$ au). The CHO bond angles are in the range of *125.1–165.5*° clearly showing the nonlinear geometry of the hydrogen-bonded motifs. The change in anion type in the ionic pair with the TetPrA cation leads to a decrease in the E_{int} values in the order of anions MsO → BSu → SA (− 390.66, − 379.95 and − 369.28 kJ/mol, respectively), which is in line with the change in energy in the series of the ionic pairs of protic ILs detected above. For the latter, however, the E_{int} values are much more negative than those of the aprotic ones, which indicate strengthened ion–ion interactions in protic ILs. In ref. [53], a thorough investigation of the ionic pairs containing tertiary diethylmethylammonium and quaternary ethyltrimethylammonium cations in anion yielded similar results.

Returning to the data in Table 2, we see that the energetic stability of the formed molecular complexes is significantly influenced by the deformation of the molecules upon formation of their complex structure. This term contributes about 25–26% to the interaction energy of the complexes; thus, its

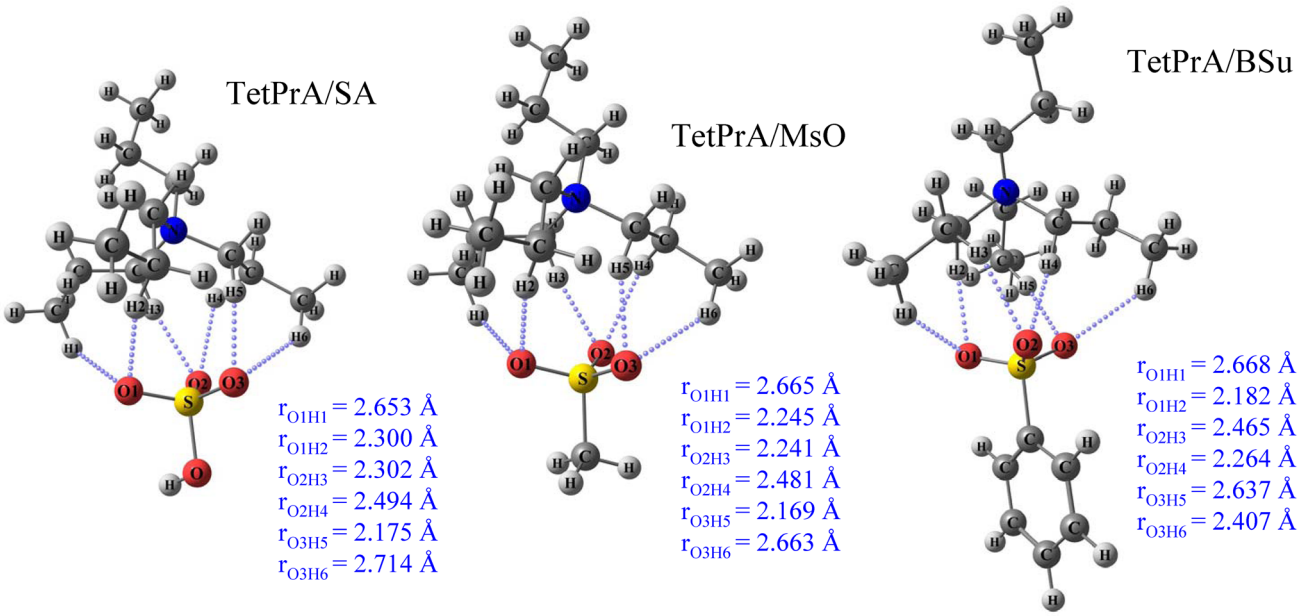

Fig. 5 Optimized geometries of the ionic pairs with quaternary tetrapropylammonium cation and different anions

contribution is very important. The considerable molecular deformation upon complex formation promotes a substantial charge transfer for the $LP_N \rightarrow BD^*_{O-H}$ donor–acceptor interactions, which, in turn, leads to the formation of the strongest hydrogen bond. And the larger the deformation energy required to form the molecular complex structure, the stronger are the hydrogen bonding interactions and the acid–base interactions in general. That was observed for hydrogen-bonded molecular complexes [54]. The deformation energies required to form the ionic structures are very similar to those found for the molecular complexes, but at the same time, their contribution is less than 5.5% of the ion–ion interaction energy. The E_{def} value for the ionic pairs would be expected to increase with the growth in the ion–ion interaction energy, as in the molecular complexes. However, the ionic pairs with the DPrA cation exhibit the smallest deformation energy among all the ionic pairs studied here, which is evidently caused by more stable ring structures with an insignificant amount of ring strain. A comparative analysis of the data shown in Table 2 reveals that the deformation energies resulting from complexation and ion pairing reduce the binding energies significantly, i.e., the values become less negative than the E_{int}. But despite this, the E_{bind} and E_{int} follow the same strength order, and both are thus appropriate for estimating the energetic stability of both the complex and the ionic pair.

The energy of hydrogen bonds (E_{HB}) is another important quantity for judging the strength of binding interactions between neutral molecules in the molecular complex or between oppositely charged ions in the ionic pair. To estimate these bond energies, there are various approaches in computational chemistry (see, e.g., refs. [55–57]). The simplest and most frequently used method of estimating the energy of hydrogen bonds is the supermolecular approach, in which the hydrogen bond energy is estimated as the difference in the energy between monomers and a hydrogen-bonded system. In the molecular hydrogen-bonded complexes mainly hydrogen bonding contributes to the binding energy between molecules, suggesting that the changes in the E_{HB} and E_{bind} values are in line with each other. By analyzing the data reported in Table 2, it can be noted that, among the two complexes of interest, PrA-MsO has a slightly larger E_{bind} than PrA-BSu. This means that the (O–)H…N hydrogen bond between the propylamine and MsO molecules in the complex is far stronger than in the case with BSu. A significant disadvantage of this method is that it is applicable only to the evaluation of the energy of a single hydrogen bond in the molecular complex. When the binding energies include not only the effects of the hydrogen bond formation but also the "pure" Coulomb attraction of two oppositely charged ions, it is very arduous to estimate the hydrogen bond energy. The main difficulty here is isolating the (N–)H...O hydrogen bonds present in the ionic pairs.

An outstanding correlation formula for predicting the E_{HB}, proposed by Espinosa et al. [58] in 1998, is based on the relationship between the potential electron energy density $V(r)$ at the bond critical point of the hydrogen bonding interaction and its corresponding energy according to the empirical expression, $E_{HB} = 1/2 \times V(r)$. Despite its popularity, this equation has numerous limitations, as discussed in [59–62], and it is safe to use for weak and moderate hydrogen bonds with $r_{HO} > 1.60$ Å and $E_{HB} < 60$ kJ/mol. Recently, Emamian et al. [63] revisited the equation of Espinosa to determine whether it really is able to predict the hydrogen bond energies with acceptable accuracy, and the results are unsatisfactory. They further put forward new empirical correlations for the molecular complexes $E_{HB} = -223.08 \times \rho(r) + 0.7423$ and for the ionic pairs $E_{HB} = -332.34 \times \rho(r) - 1.0661$. These equations have been successfully employed by several research groups for exploring the strengths of different types of hydrogen bonds in task-specific ILs [64–67].

To test the predictive power of these models, we calculated the hydrogen bond energies in the molecular complexes and ionic pairs and compared them with each other (Table 2). And, as it turned out, for molecular complexes, the hydrogen-bonded energies calculated using the Espinosa's method ($E_{HB\text{-}Espinosa}$) are significantly overestimated compared to those obtained by the Emamian's correlation (E_{HB}). Apparently, this is due to the inapplicability of the Espinosa's approach to hydrogen bonds, which are characterized by strong interaction and covalent characteristics, as mentioned above. The hydrogen bonded energies estimated by the Emamian's method are close to the binding energies in the molecular complexes. A completely different picture is observed in the ionic pairs studied here. The estimated $E_{HB\text{-}Espinosa}$ energy values are much smaller than the respective E_{HB} ones calculated by the Emamian's correlation. Although these two approaches result in very different outcomes, the order of the hydrogen bond energies in the ionic pairs in the series of the cations and anions is the same.

We found it interesting to estimate the contribution made by hydrogen bonds to the total interaction energy in each ionic pair. As it can be seen from Table 2, the sum of the energies of the two hydrogen bonds in the ionic pairs with PrA and DPrA cations is rather large; thereby, the role of hydrogen bonding in defining the ionic pair stability is all too apparent. Despite the formation of an extremely strong (N–)H…O hydrogen bond in the ionic pairs with the TPrA cation, its contribution to the ion pair stability is less than that in the ionic pairs with PrA and DPrA cations, regardless of the anion. The hydrogen bonding as a percentage of the binding energy in the ionic pairs with PrA is 21.7%, while in the ionic pairs with TPrA, it is 17.8% if the $E_{HB\text{-}Espinosa}$ values are taken into account in the calculation. A few higher energy percentages of the hydrogen bonds, ranging from 29.7 to 22.3%, are obtained from Emamian's equation because the E_{HB} values in these cases are

larger than the $E_{HB\text{-}Espinosa}$ values. Regardless of the method used to calculate E_{HB}, the hydrogen bonding interactions in the ionic pairs with the PrA cation have the highest percentage of binding energy among the ionic pairs.

Moreover, some evidence suggests that the dispersion interactions are also important for the structure of the molecular complexes [68] and ionic pairs [69–71]. To investigate this observation further, the structures presented in Fig. 1 were subjected to single-point energy calculation using the "standard" B3LYP functional with the same basis set. The difference between the interaction energy calculated using the B3LYP-GD3 method and that calculated at the B3LYP level was considered as dispersion energy (Table 2). As is seen, the dispersion interactions in the molecular complexes PrA-MsO and PrA-BSu are not much different from those in their corresponding ionic pairs. The dispersion energies in the ionic pairs with the same anion gradually increase along the sequence of PrA → DPrA → TPrA, which is quite expected if taken into account the number of propyl groups in the cation increases. A similar trend is seen among the ionic pairs with the same cation as the size of the anion grows. Also of note, the dispersion energy amounts to 4–9% of the ion–ion interaction energy, and its contribution is smaller than that of hydrogen bonding in general.

Combined with the results of our previous work [20] on studying the ionic pairs of alkylammonium–based PILs, we graphically plotted the energy of ion–ion interactions E_{int} versus the ΔPA parameter in Fig. 6. These data show that by increasing the ΔPA, the interaction between the cation and anion in the ionic pairs increases.

Recently, much attention has been paid to finding correlations between the physicochemical properties of PILs and their structural-energetic parameters derived from quantum-chemical calculations of single ionic pairs [19, 21, 52, 72–75]. Particularly, it was found that increasing the length of the alkyl radical from C1 to C4 in the alkylimidazolium cation [19] as well as replacing hydrogen atoms with alkyl groups when going from primary to tertiary ammonium cations [21, 52] results in a decrease in melting points in a series of PILs with the same anion because the interactions of the ions become weaker. For some alkylammonium PILs with different anions, it was noted a growing trend in viscosity correlated with an increase in the ion–ion interaction energy derived from the quantum chemical calculations [21, 72]. The change in melting temperature and viscosity in a series of primary ammonium PILs with thiocyanate, formate, nitrate, and hydrogen sulfate anions is the same as the change in strength of hydrogen bonds between the ions [75]. Due to the sparse experimental data, the structure–property relationship for the studied PILs cannot be established. However, as Fig. 6 shows, we can expect that low melting temperatures in combination with low viscosity and high proton conductivity will be achieved for PILs with smaller ΔPA values.

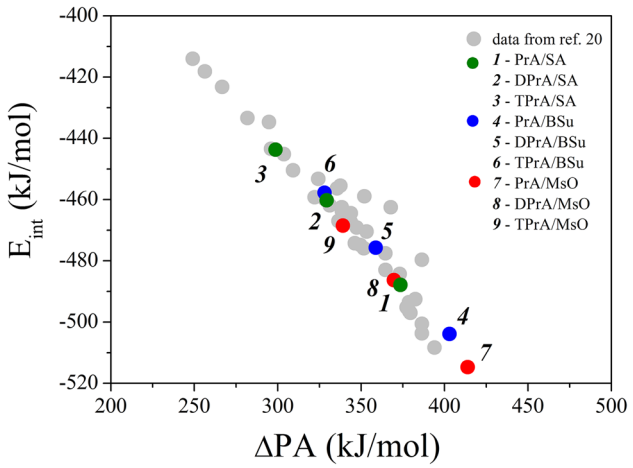

Fig. 6 Change in the energy of ion–ion interactions in the ionic pairs with the alkylammonium cation and different anions as a function of ΔPA. All data were obtained from the B3LYP-GD3/6-31++G(d,p) level

Note that the results of quantum chemical calculations do not always directly correlate with experimental data because they do not take into account the many-particle interactions caused by cations and anions in liquids. But these quantum chemical methods, in particular DFT, have been and remain an indispensable tool for the study of the IL's structure, and their use makes it possible to give a primary assessment of ion–ion interactions. They are the basis for classical molecular dynamic (MD) simulations of bulk liquids, where intramolecular and intermolecular distances, atomic charges, and energies obtained from quantum chemistry calculations are used for developing force field parameters. And, despite the discrepancy between the gas phase and real liquid, in a number of works, as noted above, it is possible to find certain correlations between the calculated and experimental data for protic ILs. MD simulations of triethylammonium-containing PILs with different anions [23] show that motifs of binding anions and cations into ion pairs, obtained by quantum-chemical calculations, are preserved in the bulk phase of the liquid. The trends in change in geometrical parameters of hydrogen bonds and the energy of ion–ion interactions in trifluoroacetate-based PILs depending on the alkylammonium cation are similar to those observed for the structures of the ion pairs obtained from the DFT method [52]. We assume that the results of our computations of the ion pairs with monopropylammonium, dipropylammonium, and tripropylammonium cations can also reflect the pattern of the bulk liquids and correlate with their physicochemical properties in a certain way.

This work is a starting point for further investigation of the structural changes when going from single ionic pairs to the bulk phase of the liquid.

Conclusions

To conclude, we have computationally studied the process of proton transfer from the acids of varying strength (benzenesulfonic (BSu), methansulfonic (MsO), and sulfuric (SA)) to the amines with different numbers of propyl substituents on the nitrogen atom (propylamine (PrA), dipropylamine (DPrA), and tripropylamine (TPrA)) upon complexation. Our results show that propylamine interacting with benzenesulfonic and methansulfonic acids can form both neutral molecular complexes and ionic pairs with hydrogen bonds. In the rest of the cases, the proton is fully transferred from the acid molecule to the amine, forming only ionic pairs. Taking into account the results from our previous quantum-chemical studies of the alkylammonium-containing ionic pairs with the different anions along with the new data, we can conclude that a larger difference in the proton affinity of the acid anion and amine is certainly not desirable for the ionic pair formations. The nature and strength of hydrogen bonding in both the molecular complexes and ionic pairs were compared. The QTAIM analysis revealed that the strength of the hydrogen bonds in the molecular complexes PrA-MsO and PrA-BSu is generally greater than that in their corresponding ionic pairs, but all of them comprise both covalent and ionic components. According to the second-perturbation energies in the NBO method, the highest values of charge transfer are along the hydrogen bond for both molecular complexes, which confirms that these bonds are more covalent in comparison with the hydrogen bonds in the ionic pairs. Among all the ionic pairs, the hydrogen bond in the ionic pairs with the TPrA cation is stronger than each of the two bonds in the ionic pairs with the PrA and DPrA cations regardless of the anion. However, there is a greater overall contribution of hydrogen bonds to the ion–ion interaction as the number of hydrogen atoms in the cation amino group increases. Good correlations of the electron density with the hydrogen bond distances and stabilization energies have been obtained. The analysis results show that the hydrogen bonding interaction in the molecular complexes contributes significantly to the energies of the acid–base interaction. For all the ionic pairs, the most important energy contribution comes from Coulomb interactions, followed by hydrogen bonding and dispersion forces. The ionic pairs with monopropylammonium, dipropylammonium, and tripropylammonium cations have stronger ion–ion interactions than ionic pairs with tetrapropylammonium (TetPrA) cation and the same anions, which further increases in the order of the cation TetPrA → TPrA → DPrA → PrA, with the sequence of anions being SA → BSu → MsO.

Author contribution IF: all quantum chemical calculations, writing—original draft, validation, visualization, conceptualization, project administration, and funding acquisition. LS: writing—review and editing.

Funding This work was supported by the Russian Science Foundation (grant no. 22-23-01155).

Data Availability All data generated or analyzed during this study are included in this published article.

Code availability Not applicable.

Declarations

Ethics approval The submission of this work is according to the ethics followed by the journal.

Consent to participate Participation was consensual.

Consent for publication All authors consent to publish.

Conflict of interest The authors declare no competing interests.

References

1. Plechkova NV, Seddon KR (2008) Application of ionic liquids in the chemical industry. Chem Soc Rev 37:123–150. https://doi.org/10.1039/B006677J
2. Stoimenovski J, Dean PM, Izgorodina EI, MacFarlane DR (2012) Protic pharmaceuticallionic liquids and solids: aspects of protonic. Faraday Discuss 154:335–352. https://doi.org/10.1039/C1FD00071C
3. Liu H, Yu H (2019) Ionic liquids for electrochemical energy storage devices applications. J Mater Sci Technol 35:674–686. https://doi.org/10.1016/j.jmst.2018.10.007
4. Elwan HA, Mamlouk M, Scott K (2021) A review of proton exchange membranes based on protic ionic liquid/polymer blends for polymer electrolyte membrane fuel cells. J Power Sources 484:229197. https://doi.org/10.1016/j.jpowsour.2020.229197
5. Vázquez-Fernández I, Raghibi M, Bouzina A, Timperman L, Bigarré J, Anouti M (2021) Protic ionic liquids/poly(vinylidene fluoride) composite membranes for fuel cell application. J Energy Chem 53:197–207. https://doi.org/10.1016/j.jechem.2020.04.022
6. Sun X-L, Deng W-H, Chen H, Han H-L, Taylor JM, Wan C-Q, Xu G (2017) A metal-organic framework impregnated with a binary ionic liquid for safe proton conduction above 100°C. Chem Eur J 23:1248–1252. https://doi.org/10.1002/chem.201605215
7. Nuthakki B, Greaves TL, Krodkiewska I, Weerawardena A, Burgar MI, Mulder RJ, Drummond CJ (2007) Protic ionic liquids and ionicity. Aust J Chem 60:21–28. https://doi.org/10.1071/CH06363
8. Greaves TL, Drummond CJ (2008) Protic ionic liquids: properties and applications. Chem Rev 108:206–237. https://doi.org/10.1021/cr068040u
9. Cruz-Cabeza AJ (2012) Acid-base crystalline complexes and the pKa rule. CrystEngComm 14:6362–6365. https://doi.org/10.1039/c2ce26055g
10. Yoshizawa M, Xu W, Angell CA (2003) Ionic liquids by proton transfer: vapor pressure, conductivity, and the relevance of ΔpKa from aqueous solutions. J Am Chem Soc 125:15411–15419. https://doi.org/10.1021/ja035783d
11. Miran MS, Kinoshita H, Yasuda T, Susan MABH, Watanabe M (2011) Hydrogen bonds in protic ionic liquids and their

correlation with physicochemical properties. Chem Commun 47:12676–12678. https://doi.org/10.1039/c1cc14817f
12. Miran MS, Kinoshita H, Yasuda T, Susan MABH, Watanabe M (2012) Physicochemical properties determined by ΔpKa for protic ionic liquids based on an organic super-strong base with various brønsted acids. Phys Chem Chem Phys 14:5178–5186. https://doi.org/10.1039/c2cp00007e
13. Stoimenovski J, Izgorodina EI, MacFarlane DR (2010) Ionicity and proton transfer in protic ionic liquids. Phys Chem Chem Phys 12:10341–10347. https://doi.org/10.1039/c0cp00239a
14. Reid JESJ, Bernardes CES, Agapito F, Martins F, Shimizu S, Minas da Piedade ME, Walker AJ (2017) Structure-property relationships in protic ionic liquids: a study of solvent-solvent and solvent-solute interactions. Phys Chem Chem Phys 19:28133–28138. https://doi.org/10.1039/c7cp05076c
15. Pant R, Kumar M, Venkatnathan A (2017) Quantum mechanical investigation of proton transport in imidazolium methanesulfonate ionic liquid. J Phys Chem C 121:7069–7080. https://doi.org/10.1021/acs.jpcc.6b11997
16. Nasrabadi AT, Gelb LD (2018) How proton transfer equilibria influence ionic liquid properties: molecular simulations of alkylammonium acetates. J Phys Chem B 122:5961–5971. https://doi.org/10.1021/acs.jpcb.8b01631
17. Ingenmey J, Gehrke S, Kirchner B (2018) How to harvest grotthuss diffusion in protic ionic liquid electrolyte systems. ChemSusChem 11:1900–1910. https://doi.org/10.1002/cssc.201800436
18. Davidowski SK, Thompson F, Huang W, Hasani M, Amin SA, Angell CA, Yarger JL (2016) NMR characterization of ionicity and transport properties for a series of diethylmethylamine based protic ionic liquids. J Phys Chem B 120:4279–4285. https://doi.org/10.1021/acs.jpcb.6b01203
19. Shmukler LE, Fedorova IV, Fadeeva YA, Gruzdev MS, Safonova LP (2022) Alkylimidazolium protic ionic liquids: structural features and physicochemical properties. ChemPhysChem 16:e202100772. https://doi.org/10.1002/cphc.202100772
20. Fedorova IV, Yablokov ME, Safonova LP (2022) Quantum-chemical study of acid-base interaction between alkylamines and different brønsted acids. Russ J Phys Chem A 96:2704–2711. https://doi.org/10.1134/S003602442212010X
21. Shmukler LE, Fedorova IV, Fadeeva YA, Safonova LP (2021) The physicochemical properties and structure of alkylammonium protic ionic liquids of $R_nH_{4-n}NX$ (n=1–3) family. a mini-review. J Mol Liq 321:114350. https://doi.org/10.1016/j.molliq.2020.114350
22. Sun X, Cao B, Zhou X, Liu S, Zhu X, Fu H (2016) Theoretical and experimental studies on proton transfer in acetate-based protic ionic liquids. J Mol Liq 221:254–261. https://doi.org/10.1016/j.molliq.2016.05.080
23. Bodo E, Bonomo M, Mariani A (2021) Assessing the structure of protic ionic liquids based on triethylammonium and organic acid anions. J Phys Chem B 125:2781–2792. https://doi.org/10.1021/acs.jpcb.1c00249
24. Fedorova IV, Krestyaninov MA, Safonova LP (2017) Ab initio study of structural features and H-bonding in alkylammonium-based protic ionic liquids. J Phys Chem A 121:7675–7683. https://doi.org/10.1021/acs.jpca.7b05393
25. Palumbo O, Cimini A, Trequattrini F, Brubach J-B, Roy P, Paolone A (2020) The infrared spectra of protic ionic liquids: performances of different computational models to predict hydrogen bonds and conformer evolution. Phys Chem Chem Phys 22:7497–7506. https://doi.org/10.1039/D0CP00907E
26. Han J, Wang L, Zhang H, Su Q, Zhou X, Liu S (2020) Determinant factor for thermodynamic stability of sulfuric acid-amine complexes. J Phys Chem A 124:10246–10257. https://doi.org/10.1021/acs.jpca.0c07908
27. Chipanina NN, Aksamentova TN, Adamovich SN, Alabanov AI, Mirskova AN, Mirskov RG, Voronkov MG (2012) The proton transfer and hydrogen bonding complexes of (2-hydroxyethyl) amines with acids: a theoretical study. Comp Theor Chem 985:36–45. https://doi.org/10.1016/j.comptc.2012.01.033
28. Verma PL, Gejji SP (2018) Modeling protic dicationic ionic liquids based on quaternary ammonium, imidazolium or pyrrolidinium cations and bis(trifluoromethanesulfonyl)imide anion: structure and spectral characteristics. J Mol Graph Model 85:304–315. https://doi.org/10.1016/j.jmgm.2018.09.010
29. Fedorova IV, Shmukler LE, Fadeeva YA, Gruzdev MS, Safonova LP (2023) On structure and properties of tripropylammonium-based protic ionic liquids with bis(trifluoromethylsulfonyl)imide and hydrogen sulfate anions. Ionics 29:661–674. https://doi.org/10.1007/s11581-022-04844-5
30. Wang C, Guo L, Li H, Wang Y, Weng J, Wu L (2006) Preparation of simple ammonium ionic liquids and their application in the cracking of dialkoxypropanes. Green Chem 8:603–607. https://doi.org/10.1039/B600041J
31. Frisch MJ, Trucks GW, Schlegel HB, Scuseria GE, Robb MA, Cheeseman JR, Scalmani G, Barone V, Mennucci B, Petersson GA, Nakatsuji H, Caricato M, Li X, Hratchian HP, Izmaylov AF, Bloino J, Zheng G, Sonnenberg JL, Hada M et al (2009) Gaussian 09, revision A.01. Gaussian, Inc., Wallingford
32. Boys S, Bernardi F (2002) The calculation of small molecular interactions by the differences of separate total energies. Some procedures with reduced errors. Mol Phys 19:553–566. https://doi.org/10.1080/00268977000101561
33. Keith TA (2010) AIMAll, version 10.05.04 (aim.tkgristmill.com)
34. Glendening ED, Reed AE, Carpenter JE, Weinhold F (2013) NBO, version 3.1.
35. Dean JA (1998) Lange's Handbook of Chemistry15th edn. McGraw-Hill, London
36. Covington AK, Thompson R (1974) Ionization of moderately strong acids in aqueous solution. Part III. Methane-, ethane-, and propanesulfonic acids at 25°C. J Solution Chem 3:603–617. https://doi.org/10.1007/BF00650404
37. Guthrie JP (1978) Hydrolysis of esters of oxy acids: pK_a values for strong acids; Brønsted relationship for attack of water at methyl; free energies of hydrolysis of esters of oxy acids; and a linear relationship between free energy of hydrolysis and pK_a holding over a range of 20 pK units. Can J Chem 56:2342–2354. https://doi.org/10.1139/v78-385
38. Low K, Tan SYS, Izgorodina EI (2019) An ab initio study of the structure and energetics of hydrogen bonding in ionic liquids. Front Chem 7:1–16. https://doi.org/10.3389/fchem.2019.00208
39. Bondi A (1964) Van der Waals volumes and radii. J Phys Chem 68:441–451. https://doi.org/10.1021/j100785a001
40. Arunan E, Desiraju GR, Klein RA, Sadlej J, Scheiner S, Alkorta I, Clary DC, Crabtree RH, Dannenberg JJ, Hobza P, Kjaergaard HG, Legon AC, Mennucci B, Nesbitt DJ (2011) Definition of the hydrogen bond (IUPAC Recommendations 2011). Pure Appl Chem 83:1637–1641. https://doi.org/10.1351/PAC-REC-10-01-02
41. Grabowski SJ (2006) Theoretical studies of strong hydrogen bonds. Annu Rep Prog Chem Sect C: Phys Chem 102:131–165. https://doi.org/10.1039/b417200k
42. Fedorova IV, Safonova LP (2020) Ion pair structures and hydrogen bonding in R_nNH_{4-n} alkylammonium ionic liquids with hydrogen sulfate and mesylate anions by DFT computations. J Phys Chem A 124:3170–3179. https://doi.org/10.1021/acs.jpca.0c01282
43. Bader RFW (1985) Atoms in molecules. Acc Chem Res 18:9–15. https://doi.org/10.1021/ar00109a003
44. Bader RFW (1990) Atoms in Molecules: A Quantum Theory. Oxford University Press, Oxford

45. Bader RFW (1991) A quantum theory of molecular structure and its applications. Chem Rev 91:893–928. https://doi.org/10.1021/cr00005a013
46. Verma PL, Gejji SP (2019) Electronic structure and spectral characteristics of alkyl substituted imidazolium based dication-X_2 (X=Br, BF_4, PF_6 and CF_3SO_3) complexes from theory. J Mol Liq 293:111548. https://doi.org/10.1016/j.molliq.2019.111548
47. Shakourian-Fard M, Fattahi A, Bayat A (2012) Ionic liquid based on α-amino acid anion and N7, N9- dimethylguaninium cation ([dMG][AA]): theoretical study on the structure and electronic properties. J Phys Chem A 116:5436–5444. https://doi.org/10.1021/jp211774y
48. Bader RFW, Essen HJ (1984) The characterization of atomic interactions. J Chem Phys 80:1943–1960. https://doi.org/10.1063/1.446956
49. Cremer D, Kraka E (1984) Chemical bonds without bonding electron density - does the difference electron-density analysis suffice for a description of the chemical bond? Angew Chem Int Ed Engl 23:627–628. https://doi.org/10.1002/anie.198406271
50. Weinhold F, Landis C (2005) Valency and bonding: a natural bond orbital donor-acceptor perspective. Cambridge University Press, New York
51. Weinhold F (1997) Nature of H-bonding in clusters, liquids, and enzymes: an ab initio, natural bond orbital perspective. J Mol Struct THEOCHEM 398:181–197. https://doi.org/10.1016/S0166-1280(96)04936-6
52. Fedorova IV, Krestyaninov MA, Safonova LP (2021) Structure and ion-ion interactions in trifluoroacetate-based ionic liquids: quantum chemical and molecular dynamics simulation studies. J Mol Liq 328:115449. https://doi.org/10.1016/j.molliq.2021.115449
53. Tsuzuki S, Shinoda W, Miran MS, Kinoshita H, Yasuda T, Watanabe M (2013) Interaction in ion pairs of protic ionic liquids: comparision with aprotic ionic liquids. J Chem Phys 139:174504. https://doi.org/10.1063/1.4827519
54. Grabowski SJ, Sokalski WA (2005) Different types of hydrogen bonds: correlation analysis of interaction energy components. J Phys Org Chem 18:779–784. https://doi.org/10.1002/poc.937
55. Keutsch FN, Cruzan JD, Saykally RJ (2003) The water trimer. Chem Rev 103:2533–2578. https://doi.org/10.1021/cr980125a
56. Munshi P, Row TNG (2005) Exploring the lower limit in hydrogen bonds: analysis of weak C− H...O and C− H... π interactions in substituted coumarins from charge density analysis. J Phys Chem A 109:659–672. https://doi.org/10.1021/jp046388s
57. Deshmukh MM, Gadre SR (2021) Molecular tailoring approach for the estimation of intramolecular hydrogen bond energy. Molecules 26:2928. https://doi.org/10.3390/molecules26102928
58. Espinosa E, Molins E, Lecomte C (1998) Hydrogen bond strengths revealed by topological analyses of experimentally observed electron densities. J Chem Phys Lett 285:170–173. https://doi.org/10.1016/S0009-2614(98)00036-0
59. Bartashevich EV, Nikulov DK, Vener MV, Tsirelson VG (2011) QTAIMC study of the X-H/H…O bond order indices (X = O, N, C) in molecular systems. Comput Theor Chem 973:33–39. https://doi.org/10.1016/j.comptc.2011.06.025
60. Bankiewicz B, Matczak P, Palusiak M (2012) Electron density characteristics in bond critical point (QTAIM) versus interaction energy components (SAPT): the case of charge-assisted hydrogen bonding. J Phys Chem A 116:452–459. https://doi.org/10.1021/jp210940b
61. Nikolaienko TY, Bulavin LA, Hovorun DM (2012) Bridging QTAIM with vibrational spectroscopy: the energy of intramolecular hydrogen bonds in DNA-related biomolecules. Phys Chem Chem Phys 14:7441–7447. https://doi.org/10.1039/C2CP40176B
62. Jabłonski M, Monaco G (2013) Different zeroes of interaction energies as the cause of opposite results on the stabilizing nature of C-H…O intramolecular interactions. J Chem Inf Model 53:1661–1675. https://doi.org/10.1021/ci400085t
63. Emamian S, Lu T, Kruse H, Emamian H (2019) Exploring nature and predicting strentgh of hydrogen bonds: a correlation analysis between atoms-in-molecules descriptors, binding energies, and energy components of symmetry-adapted perturbation theory. J Comput Chem 40:2868–2881. https://doi.org/10.1002/jcc.26068
64. Sanchora P, Pandey DK, Kagdada HL, Materny A, Singh DK (2020) Impact of alkyl chain length and water on the structure and properties of 1-alkyl-3-methylimidazolium chloride ionic liquids. Phys Chem Chem Phys 22:17687–17704. https://doi.org/10.1039/d0cp01686a
65. Agwupuye JA, Louis H, Unimuke TO, David P, Ubana EI, Moshood YL (2021) Electronic structure investigation of the stability, reactivity, NBO analysis, thermodynamics, and the nature of the interactions in methylsubstituted imidazolium-based ionic liquids. J Mol Liquids 337:116458. https://doi.org/10.1016/j.molliq.2021.116458
66. Jiang Y, Wanga Z, Lei Z, Yu G (2021) Structural effects on thermodynamic behavior and hydrogen bond interactions of water–ionic liquid systems. Chem Eng Sci 230:116186. https://doi.org/10.1016/j.ces.2020.116186
67. Li C, He H, Hou C, He M, Jiao C, Pan Q, Zhang M (2022) A quantum-chemistry and molecular-dynamics study o f non-covalent interactions between tri -n-butyl phosphate and 1-butyl-3-methylimidazolium bis(trifluoromethylsulfonyl)imide. J Mol Liquids 360:119430. https://doi.org/10.1016/j.molliq.2022.119430
68. Guttmann R, Sax AF (2017) Dispersion interactions and the stability of amine dimers. ChemistryOpen 6:571–584. https://doi.org/10.1002/open.201700052
69. Izgorodina EI, MacFarlane DR (2011) Nature of hydrogen bonding in charged hydrogen-bonded complexes and imidazolium-based ionic liquids. J Phys Chem B 115:14659–14667. https://doi.org/10.1021/jp208150b
70. Ludwig R (2015) The effect of dispersion forces on the interaction energies and far infrared spectra of protic ionic liquids. Phys Chem Chem Phys 17:13790–13793. https://doi.org/10.1039/C5CP00885A
71. Fumino K, Fossog V, Stange P, Paschek D, Hempelmann R, Ludwig R (2015) Controlling the subtle energy balance in protic ionic liquids: dispersion forces complete with hydrogen bonds. Angew Chem Int Ed 54:2792–2795. https://doi.org/10.1002/anie.201411509
72. Wei Y, Xu T, Zhang X, Di Y, Zhang Q (2018) Thermodynamic properties and intermolecular interactions of a series of n-butylammonium carboxylate ionic liquids. J Chem Eng Data 63:4475–4483. https://doi.org/10.1021/acs.jced.8b00583
73. Markusson H, Belieres JP, Johansson P, Angell CA, Jacobsson P (2007) Prediction of macroscopic properties of protic ionic liquids by ab initio calculations. J Phys Chem A 111:8717–8723. https://doi.org/10.1021/jp072036k
74. Reid JESJ, Agapito F, Bernardes CES, Martins F, Walker AJ, Shimizu S, Minas da Piedade ME (2017) Structure–property relationships in protic ionic liquids: a thermochemical study. Phys Chem Chem Phys 19:19928–19936. https://doi.org/10.1039/c7cp02230a
75. Hayes R, Imberti S, Warr GG, Atkin R (2013) The nature of hydrogen bonding in protic ionic liquids. Angew Chem Int Ed 52:4623–4627. https://doi.org/10.1002/anie.201209273

Publisher's note Springer Nature remains neutral with regard to jurisdictional claims in published maps and institutional affiliations.

Springer Nature or its licensor (e.g. a society or other partner) holds exclusive rights to this article under a publishing agreement with the author(s) or other rightsholder(s); author self-archiving of the accepted manuscript version of this article is solely governed by the terms of such publishing agreement and applicable law.